Numerische
Mathematik

CrossMark

A non-symmetric coupling of the finite volume method and the boundary element method

Christoph Erath[1] · Günther Of[2] ·
Francisco-Javier Sayas[3]

Abstract As model problem we consider the prototype for flow and transport of a concentration in porous media in an interior domain and couple it with a diffusion process in the corresponding unbounded exterior domain. To solve the problem we develop a new non-symmetric coupling between the vertex-centered finite volume and boundary element method. This discretization provides naturally conservation of local fluxes and with an upwind option also stability in the convection dominated case. We aim to provide a first rigorous analysis of the system for different model parameters; stability, convergence, and a priori estimates. This includes the use of an implicit stabilization, known from the finite element and boundary element method coupling. Some numerical experiments conclude the work and confirm the theoretical results.

Mathematics Subject Classification 65N08 · 65N38 · 65N12 · 65N15

✉ Christoph Erath
erath@mathematik.tu-darmstadt.de

Günther Of
of@tugraz.at

Francisco-Javier Sayas
fjsayas@math.udel.edu

[1] Department of Mathematics, TU Darmstadt, Dolivostraße15, 64293 Darmstadt, Germany

[2] TU Graz, Steyrergasse 30, 8010 Graz, Austria

[3] University of Delaware, 532 Ewing Hall, Newark 19716, USA

1 Model problem and introduction

Throughout this work, let $\Omega \subset \mathbb{R}^d$, $d = 2, 3$, be a bounded domain with connected polygonal Lipschitz boundary Γ and $\Omega_e = \mathbb{R}^d \backslash \overline{\Omega}$ is the corresponding unbounded exterior domain. We consider the same model problem as in [11,12]: find u and u_e such that

$$
\begin{align}
\text{div}\,(-\mathbf{A}\nabla u + \mathbf{b}u) + cu &= f && \text{in } \Omega, && \text{(1a)} \\
-\Delta u_e &= 0 && \text{in } \Omega_e, && \text{(1b)} \\
u_e(x) &= C_\infty \log|x| + \mathcal{O}(1/|x|) && \text{for } |x| \to \infty, \quad d = 2, && \text{(1c)} \\
u_e(x) &= \mathcal{O}(1/|x|) && \text{for } |x| \to \infty, \quad d = 3, && \text{(1d)} \\
u &= u_e + u_0 && \text{on } \Gamma, && \text{(1e)} \\
(\mathbf{A}\nabla u - \mathbf{b}u) \cdot \mathbf{n} &= \frac{\partial u_e}{\partial \mathbf{n}} + t_0 && \text{on } \Gamma^{in}, && \text{(1f)} \\
(\mathbf{A}\nabla u) \cdot \mathbf{n} &= \frac{\partial u_e}{\partial \mathbf{n}} + t_0 && \text{on } \Gamma^{out}, && \text{(1g)}
\end{align}
$$

where $\mathbf{A}$ is a symmetric diffusion matrix, $\mathbf{b}$ is a possibly dominating velocity field, c is a reaction function, f is a source term, and C_∞ is an unknown constant. The coefficients are allowed to be variable. The coupling boundary $\Gamma = \partial \Omega = \partial \Omega_e$ is divided in an inflow and outflow part, namely $\Gamma^{in} := \left\{x \in \Gamma \,\middle|\, \mathbf{b}(x) \cdot \mathbf{n}(x) < 0\right\}$ and $\Gamma^{out} := \left\{x \in \Gamma \,\middle|\, \mathbf{b}(x) \cdot \mathbf{n}(x) \geq 0\right\}$, respectively, where $\mathbf{n}$ is the normal vector on Γ pointing outward with respect to Ω. We allow prescribed jumps u_0 and t_0 on Γ. The radiation condition for the two dimensional case, which will be complemented with the additional hypothesis that the diameter of Ω is less than one, guarantees that our problem has a unique solution. Other radiation conditions are also possible, but some lead to restrictions on the data. Changing from one to the other is a relatively simple exercise adding sources. See [9,21] for more information on radiation conditions.

The model problem in the interior domain Ω is the prototype for flow and transport of a concentration in porous media. Usually, boundary values such as Dirichlet and/or Neumann boundary conditions are needed to solve the problem. These problems are often convection dominated and the conservation law, e.g., local conservation of fluxes, should also be preserved for a numerical approximation of the solution. Therefore, a finite volume method (FVM) is often the method of choice since it provides an easy option to stabilize the convection term and it natural preserves conservation of numerical fluxes due to its formulation. However, if the domain is unbounded, one would have to truncate the domain. The above formulation solves also another issue, i.e., if we do not know any boundary conditions, we assume a diffusion process in the corresponding (unbounded) exterior domain Ω_e, which "replaces" the boundary values. The method of choice for unbounded domains is the boundary element method (BEM), which reduces the discretization to the boundary and therefore avoids the truncation of Ω_e. Therefore, we consider an FVM–BEM coupling as in [10–12]. To the best of the authors knowledge, these works are the first theoretical justifications of a FVM–BEM coupling, where a three field coupling approach is used with either the

vertex-centered (finite volume element method, box method) FVM or the cell-centered FVM.

In this work we analyze and verify a non-symmetric FVM–BEM coupling with the vertex-centered FVM, in the following only named FVM. The main motivation of using this is to get an easier coupling formulation and a smaller system of linear equations, which saves computational costs. The idea of a non-symmetric coupling approach goes back to [3,20]. This coupling formulation applied for a finite element method (FEM)–BEM discretization is also known as Johnson–Nédélec coupling. However, the analysis in this early works relied on specific choices of the discretization spaces or on the compactness of a certain integral operator, which was in fact a restriction to a smooth boundary. In particular, a rigorous mathematical analysis for Lipschitz domains was not known. Recently, the work in [25] provided a first analysis, which overcame these restrictions. Meanwhile, several extensions and simplifications are possible, such that a SIAM review paper [26] was published. Among these extensions there are results on the non-symmetric formulation for the potential equation with variable coefficients [22,27], non-linearities [1,16], for elasticity [16,28], and for boundary value problems [17,23]. In addition, similar results have been reported on related coupling formulations [1,17] and the DG-BEM coupling [19]. We want to mention that the counterpart to the non-symmetric coupling is the symmetric coupling first introduced in [7]. However, symmetry is referred to a diffusion–diffusion transmission problem, i.e., the whole system is symmetric. We stress that this would be destroyed if one applies convection in the interior domain.

There exist a couple of papers, which analyze the vertex-centered FVM, e.g., [2,18] to mention only the very first works. It is well known that for pure diffusion with piecewise constant diffusion coefficient on a primal mesh the standard FEM and the FVM bilinear form are exactly the same. Thus the schemes differ basically only on the right-hand side. However, for all other diffusion problems [4] and a possible convection field and a reaction term the systems are different. Contrary to standard FEM, FVM still provides local flux conservation due to its formulation and provides an easy upwind stability option for convection dominated problems. The standard analysis approach makes use of a comparison between the FEM and FVM bilinear form [2,4,5,15,18]. For our FVM–BEM coupling we may apply similar techniques for the FVM part. Note that contrary to a classical FEM–BEM coupling we do not have a classical Galerkin orthogonality property due to the FVM formulation based on the conservation law. Thus the analysis differs significantly to an FEM–BEM analysis. However, we use the equivalent formulation of a stabilized continuous coupling formulation, extended here for the convection–diffusion–reaction problem in Ω, and compute an ellipticity constant. Based on the continuous stabilization we introduce a stabilization for the FVM–BEM coupling. This is needed for pure diffusion models and for convection–diffusion–reaction problems, where the energy norm reduced to a semi-norm. We stress that the stabilization is only needed for theoretical purposes since the formulation is equivalent to the standard system. We aim to provide a discrete ellipticity estimate, convergence, and a priori estimates for the FVM–BEM coupling. Our new analysis technique gives us a recipe for the coupling of BEM with a non-Galerkin method like FVM. Furthermore, this work improves the results in [10,11] for a three field FVM–BEM coupling, where we had to assume a little bit more regularity on the unknown

exterior conormal solution and some constraints on the convection and reaction terms for some special model problem configurations. However, as for the non-symmetric FEM–BEM coupling we have a theoretical constraint on the eigenvalues of $\mathbf{A}$, which is not needed in [10,11].

Throughout, we denote by $L^m(\cdot)$ and $H^m(\cdot)$, $m > 0$ the standard Lebesgue and Sobolev spaces equipped with the usual norms $\| \cdot \|_{L^2(\cdot)}$ and $\| \cdot \|_{H^m(\cdot)}$, respectively. For $\omega \subset \Omega$, $(\cdot, \cdot)_\omega$ is the L^2 scalar product. The space $H^{m-1/2}(\Gamma)$ is the space of all traces of functions from $H^m(\Omega)$ and the duality between $H^m(\Gamma)$ and $H^{-m}(\Gamma)$ is given by the extended L^2-scalar product $\langle \cdot, \cdot \rangle_\Gamma$. The space $H^1_{\ell oc}(\Omega) := \{v : \Omega \to \mathbb{R} \,|\, v|_K \in H^1(K), \text{ for all } K \subset \Omega \text{ open and bounded}\}$ collects functions with local H^1 behavior. Furthermore, the Sobolev space $W^{1,\infty}$ contains exactly the Lipschitz continuous functions. If it is clear from the context, we do not use a notational difference for functions in a domain and its traces. To simplify the presentation we equip the space $\mathcal{H} := H^1(\Omega) \times H^{-1/2}(\Gamma)$ with the norm

$$\|\mathbf{v}\|_{\mathcal{H}}^2 := \|v\|_{H^1(\Omega)}^2 + \|\psi\|_{H^{-1/2}(\Gamma)}^2$$

for $\mathbf{v} = (v, \psi) \in \mathcal{H}$.

With this notation we can specify the model data as: the diffusion matrix $\mathbf{A} : \Omega \to \mathbb{R}^{d \times d}$ has entries in $W^{1,\infty}(T)$ for all $T \in \mathcal{T}$, where $\mathcal{T}$ denotes the triangulation of Ω introduced in Sect. 3.1. Furthermore, $\mathbf{A}$ is bounded, symmetric and uniformly positive definite, i.e., there exist positive constants $C_{\mathbf{A},1}$ and $C_{\mathbf{A},2}$ with $C_{\mathbf{A},1}|\mathbf{v}|^2 \leq \mathbf{v}^T \mathbf{A}(x)\mathbf{v} \leq C_{\mathbf{A},2}|\mathbf{v}|^2$ for all $\mathbf{v} \in \mathbb{R}^d$ and almost all $x \in \Omega$. Note that these assumptions include $\mathbf{A}$ with coefficients that are $\mathcal{T}$-piecewise constant. The best constant $C_{\mathbf{A},1}$ equals the infimum over $x \in \Omega$ of the minimum eigenvalue of $\mathbf{A}(x)$, which we will denote $\lambda_{\min}(\mathbf{A})$. Furthermore, $\mathbf{b} \in W^{1,\infty}(\Omega)^d$ and $c \in L^\infty(\Omega)$ satisfy

$$\gamma(x) := \frac{1}{2}\text{div } \mathbf{b}(x) + c(x), \qquad \gamma(x) \geq 0 \quad \text{for almost every } x \in \Omega \qquad (2)$$

with the function $\gamma \in L^\infty(\Omega)$. We stress that our analysis holds for constant $\mathbf{b}$ and $c = 0$ as well. Finally, we choose the right-hand side $f \in L^2(\Omega)$, $u_0 \in H^{1/2}(\Gamma)$, and $t_0 \in H^{-1/2}(\Gamma)$. In the two dimensional case we additionally assume $\text{diam}(\Omega) < 1$ to ensure $H^{-1/2}(\Gamma)$ ellipticity of the single layer operator defined below.

Then our model problem reads in a weak sense: find $u \in H^1(\Omega)$ and $u_e \in H^1_{\ell oc}(\Omega_e)$ such that (1a)–(1g) hold.

The model problem (1) admits a unique solution for both, the two and three dimensional case [11].

Remark 1 To replace the radiation condition (1c) by $u_e(x) = \mathcal{O}(1/|x|)$ for $|x| \to \infty$ in two dimensions one would have to assume the scaling condition

$$\langle \partial u_e / \partial \mathbf{n}, 1 \rangle_\Gamma = 0$$

to guarantee solvability. As opposed for the purely diffusive case, this condition cannot be easily transformed into a condition on the data.

The content of this paper is organized as follows. Section 2 gives a short summary on integral equations and the weak formulation of our model problem based on the non-symmetric approach. We show an ellipticity estimate through an equivalent stabilized weak formulation and state the ellipticity constant explicitly. In Sect. 3 we introduce the non-symmetric FVM–BEM coupling to solve our model problem. Section 4 proves stability, convergence, and an a priori result for our coupling. Numerical experiments, found in Sect. 5, confirm the theoretical results. Some conclusions complete to work.

2 Integral equation and weak coupling formulation

The representation formula for the exterior Laplace equation (1b) with the radiation condition (1c)–(1d) and $\phi(x) = \frac{\partial}{\partial \mathbf{n}} u_e(x)|_\Gamma$, $x \in \mathbb{R}$ reads

$$u_e(x) = -\int_\Gamma G(x-y)\phi(y)\,ds_y + \int_\Gamma \frac{\partial}{\partial \mathbf{n}_y} G(x-y)u_e(y)|_\Gamma\,ds_y \qquad (3)$$

with the fundamental solution for the Laplace operator

$$G(z) := \begin{cases} -\frac{1}{2\pi}\log|z| & \text{for } z \in \mathbb{R}^2\backslash\{0\}, \\ \frac{1}{4\pi}\frac{1}{|z|} & \text{for } z \in \mathbb{R}^3\backslash\{0\}. \end{cases}$$

From (3) we obtain (taking traces) the boundary integral equation on Γ

$$u_e|_\Gamma = (1/2 + \mathcal{K})u_e|_\Gamma - \mathcal{V}\phi. \qquad (4)$$

The single layer operator $\mathcal{V}$ and the double layer operator $\mathcal{K}$ are given, for smooth enough input, by

$$(\mathcal{V}\psi)(x) = \int_\Gamma \psi(y)G(x-y)\,ds_y, \quad (\mathcal{K}\theta)(x) = \int_\Gamma \theta(y)\frac{\partial}{\partial \mathbf{n}_y}G(x-y)\,ds_y, \qquad x \in \Gamma,$$

where $\mathbf{n}_y$ is a normal vector with respect to y. The integral equation (4) holds on Γ except on corners and edges. We recall [8, Theorem 1] that these operators can be extended to bounded operators

$$\mathcal{V} \in L\left(H^{s-1/2}(\Gamma); H^{s+1/2}(\Gamma)\right), \quad \mathcal{K} \in L\left(H^{s+1/2}(\Gamma); H^{s+1/2}(\Gamma)\right), \quad s \in \left[-\tfrac{1}{2}, \tfrac{1}{2}\right].$$

It is also well-known that $\mathcal{V}$ is symmetric and $H^{-1/2}(\Gamma)$ elliptic, since we additionally assume $\operatorname{diam}(\Omega) < 1$ in the two dimensional case, which can always be achieved by scaling. The expressions

$$\|\cdot\|_{\mathcal{V}}^2 := \langle\mathcal{V}\cdot,\cdot\rangle_\Gamma, \qquad \|\cdot\|_{\mathcal{V}^{-1}}^2 := \langle\cdot,\mathcal{V}^{-1}\cdot\rangle_\Gamma$$

define norms in $H^{-1/2}(\Gamma)$ and $H^{1/2}(\Gamma)$, respectively. These norms are equivalent to the usual ones.

We consider a weak form of the model problem (1) in terms of boundary integral operators. For that we use the non-symmetric approach, i.e, calculate the weak formulation of the interior problem and replace the interior conormal derivative by the exterior $\phi := \partial u_e / \partial \mathbf{n}|_\Gamma$ and the corresponding jump relations t_0, (1f)–(1g). Second, we take the weak form of (4) and replace the exterior trace $u_e|_\Gamma$ by the interior trace $u_{|\Gamma}$ and the jump u_0, (1e). Then the coupling reads: find $u \in H^1(\Omega)$, $\phi \in H^{-1/2}(\Gamma)$ such that

$$\mathcal{A}(u, v) - \langle \phi, v \rangle_\Gamma = (f, v)_\Omega + \langle t_0, v \rangle_\Gamma, \tag{5a}$$

$$\langle \psi, (1/2 - \mathcal{K})u \rangle_\Gamma + \langle \psi, \mathcal{V}\phi \rangle_\Gamma = \langle \psi, (1/2 - \mathcal{K})u_0 \rangle_\Gamma \tag{5b}$$

for all $v \in H^1(\Omega)$, $\psi \in H^{-1/2}(\Gamma)$. The bilinear form in (5a) is given by

$$\mathcal{A}(u, v) := (\mathbf{A}\nabla u - \mathbf{b}u, \nabla v)_\Omega + (cu, v)_\Omega + \langle \mathbf{b} \cdot \mathbf{n} \, u, v \rangle_{\Gamma^{out}}.$$

Lemma 1 *The bilinear form $\mathcal{A}$ is coercive (in the $H^1(\Omega)$ norm and $H^1(\Omega)$ semi-norm, respectively) and continuous on $H^1(\Omega) \times H^1(\Omega)$, i.e., for all $v, w \in H^1(\Omega)$ and $\gamma(x)$ from assumption (2) there holds*

$$\mathcal{A}(v, v) \geq \begin{cases} C_{\mathcal{A},1} \|v\|^2_{H^1(\Omega)} & \text{for } \gamma(x) > 0 \text{ almost everywhere in } \Omega, \\ C^\star_{\mathcal{A},1} \|v\|^2_{H^1(\Omega)} & \text{for } \gamma(x) > 0 \text{ on } \omega \subsetneq \Omega, \, |\omega| > 0, \, \gamma(x) = 0 \text{ elsewhere}, \\ C'_{\mathcal{A},1} \|\nabla v\|^2_{L^2(\Omega)} & \text{for } \gamma(x) = 0 \text{ almost everywhere in } \Omega, \end{cases} \tag{6}$$

$$|\mathcal{A}(w, v)| \leq C_{\mathcal{A},2} \|w\|_{H^1(\Omega)} \|v\|_{H^1(\Omega)}. \tag{7}$$

Here, the constants $C_{\mathcal{A},1} = \min\{\lambda_{\min}(\mathbf{A}), \inf_{x \in \Omega} \gamma(x)\} > 0$, $C'_{\mathcal{A},1} = \lambda_{\min}(\mathbf{A}) > 0$ and $C_{\mathcal{A},2} > 0$, depend on the data $\mathbf{A}$, $\mathbf{b}$ and c. The constant $C^\star_{\mathcal{A},1} = \min\{\lambda_{\min}(\mathbf{A}), C(\gamma(x), \omega, \Omega)\} > 0$ depends additionally on the constant $C(\gamma(x), \omega, \Omega) > 0$, which is not known but depends on $\gamma(x) > 0$ in ω, ω, and Ω.

Proof There holds

$$\int_{\Gamma^{out}} \mathbf{b} \cdot \mathbf{n} \, v^2 \, ds \geq \frac{1}{2} \int_\Gamma \mathbf{b} \cdot \mathbf{n} \, v^2 \, ds = \frac{1}{2} \int_\Omega \text{div} \, (\mathbf{b}v^2) \, dx$$
$$= \frac{1}{2}((\text{div } \mathbf{b})v, v)_\Omega + (\mathbf{b}v, \nabla v)_\Omega.$$

If $\frac{1}{2}\text{div } \mathbf{b}(x) + c(x) \geq \gamma(x) > 0$ of assumption (2) is positive almost everywhere in Ω, it follows that

$$\mathcal{A}(v, v) \geq (\mathbf{A}\nabla v, \nabla v)_\Omega + \frac{1}{2}((\text{div } \mathbf{b})v, v)_\Omega + (cv, v)_\Omega \geq C_{\mathcal{A},1}\|v\|^2_{H^1(\Omega)}.$$

If $\gamma(x) > 0$ holds on a set $\omega \subsetneq \Omega$ of positive measure but $\gamma(x) = 0$ on $\Omega \backslash \omega$, we can use a compactness argument (or the Deny–Lions theorem) to prove coercivity of $\mathcal{A}$ in $H^1(\Omega)$. Then the coercivity constant $C^\star_{\mathcal{A},1}$ is not known. When $\gamma(x) = 0$ almost everywhere in Ω, we only obtain coercivity of $\mathcal{A}$ with respect to the H^1 semi-norm and the constant $C'_{\mathcal{A},1}$. Using simple arguments, the continuity bound (7) can be easily proved with

$$C_{\mathcal{A},2} = 2 \max \left\{ \|\mathbf{A}\|_{L^\infty(\Omega)^{d \times d}}, \|\mathbf{b}\|_{L^\infty(\Omega)}, \|c\|_{L^\infty(\Omega)} \right\} + C_\Gamma^2 \|\mathbf{b} \cdot \mathbf{n}\|_{L^\infty(\Gamma^{out})},$$

where C_Γ is the norm of the trace operator $H^1(\Omega) \to L^2(\Gamma^{out})$. $\qquad\square$

For convenience the system (5a)–(5b) can be written in the product space $\mathcal{H} = H^1(\Omega) \times H^{-1/2}(\Gamma)$ as follows: we introduce the bilinear form $\mathcal{B} : \mathcal{H} \times \mathcal{H} \to \mathbb{R}$

$$\mathcal{B}((u, \phi); (v, \psi)) := \mathcal{A}(u, v) - \langle \phi, v \rangle_\Gamma + \langle \psi, (1/2 - \mathcal{K})u \rangle_\Gamma + \langle \psi, \mathcal{V}\phi \rangle_\Gamma, \qquad (8)$$

and the linear functional

$$F((v, \psi)) := (f, v)_\Omega + \langle t_0, v \rangle_\Gamma + \langle \psi, (1/2 - \mathcal{K})u_0 \rangle_\Gamma. \qquad (9)$$

Then (5a)–(5b) is equivalent to: find $\mathbf{u} \in \mathcal{H}$ such that

$$\mathcal{B}(\mathbf{u}; \mathbf{v}) = F(\mathbf{v}) \qquad \text{for all } \mathbf{v} \in \mathcal{H}. \qquad (10)$$

With integration by parts we calculate

$$\mathcal{B}(\mathbf{v}; \mathbf{v}) = (\mathbf{A}\nabla v, \nabla v)_\Omega + \left(\left(\tfrac{1}{2} \mathrm{div}\, \mathbf{b} + c \right) v, v \right)_\Omega - \langle \mathbf{b} \cdot \mathbf{n}\, v, v \rangle_{\Gamma^{in}} + \langle \mathbf{b} \cdot \mathbf{n}\, v, v \rangle_{\Gamma^{out}}$$
$$- \langle \psi, v \rangle_\Gamma + \langle \psi, (1/2 - \mathcal{K})v \rangle_\Gamma + \langle \psi, \mathcal{V}\psi \rangle_\Gamma,$$

and thus we see

$$\mathcal{B}((1, 0); (1, 0)) = \int_\Omega \left(\tfrac{1}{2} \mathrm{div}\, \mathbf{b} + c \right) dx + \int_\Gamma |\mathbf{b} \cdot \mathbf{n}|\, ds.$$

Thus if $\tfrac{1}{2}\mathrm{div}\, \mathbf{b} + c = 0$ in Ω and $\mathbf{b} \cdot \mathbf{n} = 0$ on Γ (in particular, when $\mathbf{b} = (0, 0)^T$ and $c = 0$), it follows that $\mathcal{B}((1, 0); (1, 0)) = 0$. This lack of coercivity will be remedied using an equivalent variational problem for the sake of analysis.

Therefore, we define the linear operator

$$P((v, \psi)) := \langle 1, (1/2 - \mathcal{K})v + \mathcal{V}\psi \rangle_\Gamma = \int_\Gamma ((1/2 - \mathcal{K})v + \mathcal{V}\psi)\, ds$$

and introduce a parameter β depending on $\gamma(x)$ of assumption (2);

$$\beta := \begin{cases} 1 & \text{if } \gamma(x) = 0 \text{ almost everywhere in } \Omega, \\ 0 & \text{else.} \end{cases} \qquad (11)$$

Then the β-dependent perturbation of the bilinear form $\mathcal{B}(\mathbf{u}, \mathbf{v})$ is

$$\widetilde{\mathcal{B}}(\mathbf{u}; \mathbf{v}) := \mathcal{B}(\mathbf{u}, \mathbf{v}) + \beta P(\mathbf{u}) P(\mathbf{v}), \tag{12}$$

and of the linear map $F(\mathbf{v})$

$$\widetilde{F}(\mathbf{v}) := F(\mathbf{v}) + \beta \langle 1, (1/2 - \mathcal{K})u_0 \rangle_\Gamma P(\mathbf{v}). \tag{13}$$

Thus a stabilized variational formulation is given by: find $\mathbf{u} \in \mathcal{H}$ such that

$$\widetilde{\mathcal{B}}(\mathbf{u}; \mathbf{v}) = \widetilde{F}(\mathbf{v}) \qquad \text{for all } \mathbf{v} \in \mathcal{H}. \tag{14}$$

Note that this type of stabilization has also been considered in [22] and [1]. We emphasize that this formulation is introduced purely for theoretical purposes, and the discretization will be applied directly on (5a)–(5b).

Lemma 2 *The variational formulation* (10) *and the stabilized version in* (14) *are equivalent.*

Proof The equivalence of formulations was stated in [1, Theorem 14] for a pure diffusion problem. The convection and reaction terms in the bilinear form $\mathcal{A}$ do not affect the proof. We note that we will see a similar result for the FVM–BEM discretization in Lemma 4. $\square$

The next theorem on the coercivity of the bilinear form $\widetilde{\mathcal{B}}$ is an extended and improved version of the one stated in [22, Theorem 3.1] and [1, Theorem 15] for a purely diffusive problem. We extend it by the convection and reaction terms in the bilinear form and present an improved ellipticity constant compared to [22, Theorem 3.1]. This is possible due to some modification of the proof inspired by [23]. Before we state the theorem, we recall an important contractivity result for the double layer operator [22, Lemma 2.1] with the contraction constant $C_\mathcal{K}$ from [29]: there exists $C_\mathcal{K} \in [1/2, 1)$ such that

$$\|(1/2 + \mathcal{K})v\|_{\mathcal{V}^{-1}}^2 \leq C_\mathcal{K} \langle \mathcal{V}^{-1}(1/2 + \mathcal{K})v, v \rangle_\Gamma. \tag{15}$$

Furthermore, we define for $\beta = 0$

$$C_{\mathbf{b}c} := \begin{cases} \inf_{x \in \Omega} \gamma(x) & \text{for } \gamma(x) > 0 \text{ almost everywhere in } \Omega, \\ C(\gamma(x), \omega, \Omega) & \text{for } \gamma(x) > 0 \text{ on } \omega \subsetneq \Omega, |\omega| > 0, \gamma(x) = 0 \text{ elsewhere} \end{cases} \tag{16}$$

with $\gamma(x)$ from assumption (2) and the unknown constant $C(\gamma(x), \omega, \Omega) > 0$ introduced in Lemma 1.

Theorem 1 *If $\lambda_{\min}(\mathbf{A}) > C_{\mathcal{K}}/4$, then $\widetilde{\mathcal{B}}$ is $\mathcal{H}$-elliptic. More precisely, for all $\mathbf{v} = (v, \psi) \in \mathcal{H}$ holds*

$$\widetilde{\mathcal{B}}(\mathbf{v}; \mathbf{v}) \geq C_{\mathrm{stab}} \left[\|\nabla v\|_{L_2(\Omega)}^2 + (1 - \beta)\|v\|_{L_2(\Omega)}^2 + \beta P(\mathbf{v})^2 + \|\psi\|_{\mathcal{V}}^2 \right]. \qquad (17)$$

The stability constant C_{stab} reads

$$C_{\mathrm{stab}} = \begin{cases} \min\left\{ C_{\mathbf{b}c}, \frac{1}{2}\left[\lambda_{\min}(\mathbf{A}) + 1 - \sqrt{(\lambda_{\min}(\mathbf{A}) - 1)^2 + C_{\mathcal{K}}} \right] \right\} & \text{for } \beta = 0, \\[2mm] \min\left\{ 1, \frac{1}{2}\left[\lambda_{\min}(\mathbf{A}) + 1 - \sqrt{(\lambda_{\min}(\mathbf{A}) - 1)^2 + C_{\mathcal{K}}} \right] \right\} & \text{for } \beta = 1 \end{cases}$$

and depends on the model data $\mathbf{A}$, $\mathbf{b}$, c, and the contraction constant $C_{\mathcal{K}}$.

Remark 2 The right-hand side in (17) defines an equivalent norm in $\mathcal{H}$. While this is obvious for $\beta = 0$, a simple compactness argument (see [1, Lemma 10 and (65)] for a similar argument) shows the equivalence for $\beta = 1$. Note that we only do not know the constant C_{stab} explicitly in the second case of (16).

Proof The proof is in the spirit of previous publications [1,22,23] on the non-symmetric FEM–BEM coupling, but extended here for the different interior model problem. Therefore, we only present the key points.

An element $v \in H^1(\Omega)$ can be decomposed as a sum $v = v_\Gamma + v_0$, where v_Γ is harmonic and $v_0 \in H_0^1(\Omega)$. Thus $(\nabla v_\Gamma, \nabla w)_\Omega = 0$ for all $w \in H_0^1(\Omega)$, which implies that

$$\|\nabla v\|_{L^2(\Omega)}^2 = \|\nabla v_0\|_{L^2(\Omega)}^2 + \|\nabla v_\Gamma\|_{L^2(\Omega)}^2 = \|\nabla v_0\|_{L^2(\Omega)}^2 + \langle S^{\mathrm{int}} v, v \rangle_\Gamma, \qquad (18)$$

where $S^{\mathrm{int}} := \mathcal{V}^{-1}(1/2 + \mathcal{K})$ denotes the Steklov–Poincaré operator, i.e., the Dirichlet to Neumann map of the interior Laplace problem. The term $\langle S^{\mathrm{int}} v, v \rangle_\Gamma$ will help to compensate possible negative contributions of the non-symmetric coupling to the total energy of the system. Let us first recall our choice of β depending on $\gamma(x)$ in (11) and the definition of $C_{\mathbf{b}c}$ in (16). This allows us to write the coercivity estimate of Lemma 1 as

$$\mathcal{A}(v, v) \geq \lambda_{\min}(\mathbf{A})\|\nabla v\|_{L^2(\Omega)}^2 + (1 - \beta)C_{\mathbf{b}c}\|v\|_{L^2(\Omega)}^2 \qquad \text{for all } v \in H^1(\Omega).$$

Following [22] and using (15), we can easily estimate

$$\begin{aligned} \langle \psi, (1/2 + \mathcal{K})v \rangle_\Gamma &= \langle \mathcal{V}\psi, \mathcal{V}^{-1}(1/2 + \mathcal{K})v \rangle_\Gamma \\ &\leq \|\mathcal{V}^{-1}(1/2 + \mathcal{K})v\|_{\mathcal{V}}\|\psi\|_{\mathcal{V}} = \|(1/2 + \mathcal{K})v\|_{\mathcal{V}^{-1}}\|\psi\|_{\mathcal{V}} \\ &\leq C_{\mathcal{K}}^{1/2}\langle S^{\mathrm{int}}v, v \rangle_\Gamma^{1/2}\|\psi\|_{\mathcal{V}} \end{aligned}$$

for all $(v, \psi) \in \mathcal{H}$. Therefore, for all $\mathbf{v} = (v, \psi) \in \mathcal{H}$, we can estimate

$$\widetilde{\mathcal{B}}(\mathbf{v}; \mathbf{v}) = \mathcal{A}(v, v) + \langle \psi, \mathcal{V}\psi \rangle_\Gamma - \langle \psi, (1/2 + \mathcal{K})v \rangle_\Gamma + \beta P(\mathbf{v})^2$$

$$\geq \lambda_{\min}(\mathbf{A})\|\nabla v\|_{L_2(\Omega)}^2 + (1-\beta)C_{\mathbf{bc}}\|v\|_{L_2(\Omega)}^2 + \beta P(\mathbf{v})^2$$
$$+ \|\psi\|_{\mathcal{V}}^2 - C_{\mathcal{K}}^{1/2}\langle S^{\text{int}}v, v\rangle_{\Gamma}^{1/2}\|\psi\|_{\mathcal{V}}$$
$$\geq \lambda_{\min}(\mathbf{A})\|\nabla v_0\|_{L_2(\Omega)}^2 + (1-\beta)C_{\mathbf{bc}}\|v\|_{L_2(\Omega)}^2 + \beta P(\mathbf{v})^2$$
$$+ \begin{pmatrix} \langle S^{\text{int}}v, v\rangle_{\Gamma}^{1/2} \\ \|\psi\|_{\mathcal{V}} \end{pmatrix}^{\top} \begin{pmatrix} \lambda_{\min}(\mathbf{A}) & -\frac{1}{2}\sqrt{C_{\mathcal{K}}} \\ -\frac{1}{2}\sqrt{C_{\mathcal{K}}} & 1 \end{pmatrix} \begin{pmatrix} \langle S^{\text{int}}v, v\rangle_{\Gamma}^{1/2} \\ \|\psi\|_{\mathcal{V}} \end{pmatrix},$$

where in the last inequality we have used the harmonic splitting (18). Since $\lambda_{\min}(\mathbf{A}) > 0$, the quadratic form in the right-hand side of the above estimate is positive definite if and only if

$$\begin{vmatrix} \lambda_{\min}(\mathbf{A}) & -\frac{1}{2}\sqrt{C_{\mathcal{K}}} \\ -\frac{1}{2}\sqrt{C_{\mathcal{K}}} & 1 \end{vmatrix} = \lambda_{\min}(\mathbf{A}) - \frac{1}{4}C_{\mathcal{K}} > 0.$$

Calculating the smallest eigenvalue of the matrix above, we can bound

$$\widetilde{\mathcal{B}}(\mathbf{v}; \mathbf{v}) \geq C_{\text{stab}}\left(\|\nabla v_0\|_{L_2(\Omega)}^2 + \langle S^{\text{int}}v, v\rangle_{\Gamma} + (1-\beta)\|v\|_{L_2(\Omega)}^2\right.$$
$$\left. + \beta P(\mathbf{v})^2 + \|\psi\|_{\mathcal{V}}^2\right),$$

which, using (18), is the estimate of the statement of the theorem.   □

Remark 3 Note that this result also improves the estimate of [22, Theorem 3.1] for a pure diffusion problem in Ω. The smallest eigenvalue in C_{stab} in the case $\beta = 1$ is observed to be sharp in the numerical experiments of [22], contrary to the constant reported therein.

Using the boundedness of $\mathcal{A}$ in (7) and mapping properties of the integral operators, it is easy to conclude that the bilinear form $\widetilde{\mathcal{B}}$ defined in (12) and the linear form $\widetilde{F}$ in (13) are bounded. Thus we can conclude the unique solvability of (14). Due to the equivalence of the formulations in Lemma 2, the original variational formulation (5a)-(5b) is uniquely solvable.

Remark 4 Note that the equivalence of (14) and (10) shown in Lemma 2 and the ellipticity estimate (17) also hold true on the discrete level, if the constants are in the discretization space of $H^{-1/2}(\Gamma)$. In other words, a possible FEM–BEM coupling solution, as shown in Remark 7, exists and is unique and the Céa Lemma applies.

3 A non-symmetric FVM–BEM coupling

In this section we develop a FVM–BEM coupling discretization in the sense of a non-symmetric coupling approach. From now on we assume $t_0 \in L^2(\Gamma)$. First, let us introduce the notation for the triangulation and some discrete function spaces.

3.1 Triangulation

Throughout, $\mathcal{T}$ denotes a triangulation or primal mesh of Ω, and $\mathcal{N}$ and $\mathcal{E}$ are the corresponding set of nodes and edges/faces, respectively. The elements $T \in \mathcal{T}$ are non-degenerate triangles (2-D case) or tetrahedra (3-D case), and considered to be closed. For the Euclidean diameter of $T \in \mathcal{T}$ we write $h_T := \sup_{x,y \in T} |x - y|$. Moreover, h_E denotes the length of an edge or Euclidean diameter of $E \in \mathcal{E}$. The triangulation is regular in the sense of Ciarlet [6], i.e., the ratio of the diameter h_T of any element $T \in \mathcal{T}$ to the diameter of its largest inscribed ball is bounded by a constant independent of h_T, the so called shape-regularity constant. Additionally, we assume that the triangulation $\mathcal{T}$ is aligned with the discontinuities of the coefficients **A**, **b**, and c of the differential equation (if any), the data f, u_0, and t_0. Throughout, if **n** appears in a boundary integral, it denotes the unit normal vector to the boundary pointing outward the domain. We denote by $\mathcal{E}_T \subset \mathcal{E}$ the set of all edges/faces of T, i.e., $\mathcal{E}_T := \{E \in \mathcal{E} \mid E \subset \partial T\}$ and by $\mathcal{E}_\Gamma := \{E \in \mathcal{E} \mid E \subset \Gamma\}$ the set of all edges/faces on the boundary Γ.

Dual mesh
We construct the dual mesh $\mathcal{T}^*$ from the primal mesh $\mathcal{T}$ as follows. In two dimensions we connect the center of gravity of an element $T \in \mathcal{T}$ with the midpoint of the edges $E \in \mathcal{E}_T$; see Fig. 1a, where the dashed lines are the new boxes, called control volumes. In three dimensions we connect the center of gravity of an element $T \in \mathcal{T}$ with the centers of gravity of the four faces $E \in \mathcal{E}_T$. Furthermore, each center of gravity of a face $E \in \mathcal{E}_T$ is connected by straight lines to the midpoints of its edges. The elements of this dual mesh $\mathcal{T}^*$ are taken to be closed. Note that they are non-degenerate domains because of the non-degeneracy of the elements of the primal mesh. Given a vertex
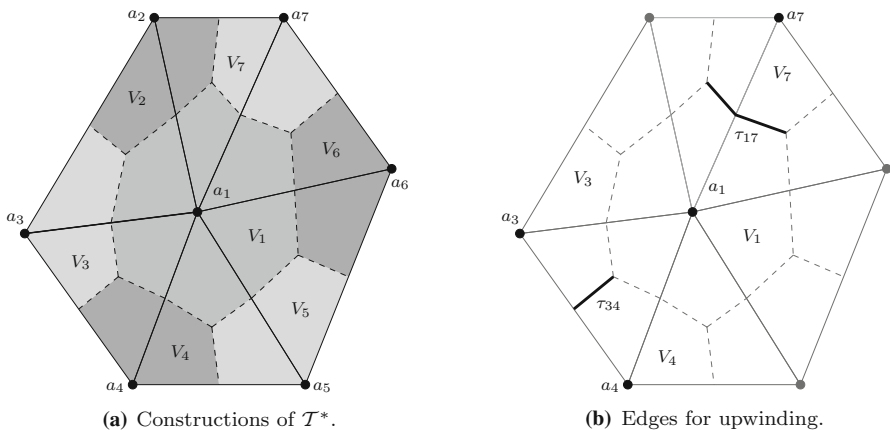

(a) Constructions of $\mathcal{T}^*$. **(b)** Edges for upwinding.

Fig. 1 The construction of the dual mesh $\mathcal{T}^*$ from the primal mesh $\mathcal{T}$ in two dimensions with the center of gravity point in the interior of the elements in (**a**); the *dashed lines* (*gray boxes*) are the new control volumes V_i of $\mathcal{T}^*$ and are associated with $a_i \in \mathcal{N}$. In (**b**) we see an example intersection $\tau_{17} = V_1 \cap V_7 \neq \emptyset$ of two neighboring cells $V_1, V_7 \in \mathcal{T}^*$, where τ_{17} is the union of two straight segments. For $a_3, a_4 \in \mathcal{N}$, where both a_3 and a_4 lie on Γ, $\tau_{34} = V_3 \cap V_4 \neq \emptyset$ is only a single segment

$a_i \in \mathcal{N}$ from the primal mesh $\mathcal{T}$ ($i = 1 \ldots \#\mathcal{N}$), there exists a unique box containing a_i. We thus number the elements of the dual mesh $V_i \in \mathcal{T}^*$, following the numbering of vertices.

Remark 5 In two dimensions, instead of starting the construction of the boxes in the center of gravity, we can use the center of the circle circumscribed to the element. Connecting these points with the midpoints of the edges we form the so called Voronoi or perpendicular bisector meshes, since the connection between to neighbor's circumscribed circle points is perpendicular to the shared edge. Our analysis works with such meshes as well.

Discrete function spaces
We define with $\mathcal{S}^1(\mathcal{T}) := \{v \in \mathcal{C}(\Omega) \,|\, v|_T$ affine for all $T \in \mathcal{T}\}$ the piecewise affine and globally continuous function space on $\mathcal{T}$. The space $\mathcal{P}^0(\mathcal{E}_\Gamma)$ is the $\mathcal{E}_\Gamma$-piecewise constant function space. On the dual mesh $\mathcal{T}^*$ we provide $\mathcal{P}^0(\mathcal{T}^*) := \{v \in L^2(\Omega) \,|\, v|_V$ constant $V \in \mathcal{T}^*\}$. With the aid of the characteristic function χ_i^* over the volume $V_i \in T\mathcal{T}^*$ we write for $v_h^* \in \mathcal{P}^0(\mathcal{T}^*)$

$$v_h^* = \sum_{x_i \in \mathcal{N}} v_i \chi_i^*,$$

with real coefficients v_i. Furthermore, we define the $\mathcal{T}^*$-piecewise constant interpolation operator

$$\mathcal{I}_h^* : \mathcal{C}(\overline{\Omega}) \to \mathcal{P}^0(\mathcal{T}^*), \quad \mathcal{I}_h^* v := \sum_{a_i \in \mathcal{N}} v(a_i) \chi_i^*(x). \tag{19}$$

Because of the construction of the dual mesh from the primal mesh and the definition of $\mathcal{I}_h^*$ there hold the well known results:

Lemma 3 *Let $T \in \mathcal{T}$ and $E \in \mathcal{E}_T$. For $v_h \in \mathcal{S}^1(\mathcal{T})$ there holds*

$$\int_E (v_h - \mathcal{I}_h^* v_h) \, ds = 0, \tag{20}$$

$$\|v_h - \mathcal{I}_h^* v_h\|_{L^2(T)} \leq h_T \|\nabla v_h\|_{L^2(T)}, \tag{21}$$

$$\|v_h - \mathcal{I}_h^* v_h\|_{L^2(E)} \leq C h_E^{1/2} \|\nabla v_h\|_{L^2(T)}, \tag{22}$$

where the constant $C > 0$ depends only on the shape regularity constant.

Proof The proofs are standard. Note that for (20) we need the fact, that the dual mesh $\mathcal{T}^*$ is constructed through the midpoint of an edge $E \in \mathcal{E}$ in the two dimensional case and the center of gravity point if E is a face in the three dimensional case. A proof of (21) can be found in [10], and (22) follows from (21) through the standard trace inequality. Note that the above statements are independent of the choice of the interior point in $T \in \mathcal{T}$ for the $\mathcal{T}^*$ construction. □

3.2 The discrete system

A classical finite volume discretization describes numerically a conservation law of the model problem, i.e., a quantity in a volume can only change due to the inflow and outflow flux balance through its boundary. More precisely, for our model problem we integrate (1a) over each dual control volume $V \in \mathcal{T}^*$ and apply the divergence theorem. If we use the transmission condition (1f)–(1g) we thus get a balance equation for the interior problem

$$\int_{\partial V \backslash \Gamma} (-\mathbf{A}\nabla u_h + \mathbf{b}u_h) \cdot \mathbf{n}\, ds + \int_V c u_h\, dx$$
$$+ \int_{\partial V \cap \Gamma^{out}} \mathbf{b} \cdot \mathbf{n}\, u_h\, ds - \int_{\partial V \cap \Gamma} \phi_h\, ds = \int_V f\, dx + \int_{\partial V \cap \Gamma} t_0\, ds \qquad (23)$$

for all $V \in \mathcal{T}^*$. Note that the discretization in the interior domain follows along the dual mesh $\mathcal{T}^*$. Here, $u_h \in \mathcal{S}^1(\mathcal{T})$ and $\phi_h \in \mathcal{P}^0(\mathcal{E}_\Gamma)$ approximate u and ϕ, respectively. We can rewrite (23) in terms of a variational formulation;

$$\mathcal{A}_V(u_h, v_h) - \langle \phi_h, \mathcal{I}_h^* v_h \rangle_\Gamma = (f, \mathcal{I}_h^* v_h)_\Omega + \langle t_0, \mathcal{I}_h^* v_h \rangle_\Gamma$$

with the finite volume bilinear form $\mathcal{A}_V : \mathcal{S}^1(\mathcal{T}) \times \mathcal{S}^1(\mathcal{T}) \to \mathbb{R}$ given by

$$\mathcal{A}_V(u_h, v_h) := \sum_{a_i \in \mathcal{N}} v_h(a_i) \left(\int_{\partial V_i \backslash \Gamma} (-\mathbf{A}\nabla u_h + \mathbf{b}u_h) \cdot \mathbf{n}\, ds \right.$$
$$\left. + \int_{V_i} c u_h\, dx + \int_{\partial V_i \cap \Gamma^{out}} \mathbf{b} \cdot \mathbf{n}\, u_h\, ds \right). \qquad (24)$$

Remark 6 Note that the trial and test spaces are different in practice. The test functions in the finite volume part are in $\mathcal{P}^0(\mathcal{T}^*)$, which is realized by taking nodal values $v_h(a_i)$ in (24) and by interpolation $\mathcal{I}_h^* v_h \in \mathcal{P}^0(\mathcal{T}^*)$ for $v_h \in \mathcal{S}^1(\mathcal{T})$. We have chosen the above definition to simplify the notation below.

To complete the coupling formulation we choose as in the classical non-symmetric FEM–BEM formulation the BEM equation (4) and replace the continuous ansatz and test spaces by discrete subspaces. Finally, the discrete system reads: find $u_h \in \mathcal{S}^1(\mathcal{T})$ and $\phi_h \in \mathcal{P}^0(\mathcal{E}_\Gamma)$ such that

$$\mathcal{A}_V(u_h, v_h) - \langle \phi_h, \mathcal{I}_h^* v_h \rangle_\Gamma = (f, \mathcal{I}_h^* v_h)_\Omega + \langle t_0, \mathcal{I}_h^* v_h \rangle_\Gamma, \qquad (25a)$$
$$\langle \psi_h, (1/2 - \mathcal{K})u_h \rangle_\Gamma + \langle \psi_h, \mathcal{V}\phi_h \rangle_\Gamma = \langle \psi_h, (1/2 - \mathcal{K})u_0 \rangle_\Gamma \qquad (25b)$$

for all $v_h \in \mathcal{S}^1(\mathcal{T})$, $\psi_h \in \mathcal{P}^0(\mathcal{E}_\Gamma)$.

As in the continuous case we write the system in a more compact way. We consider the product space $\mathcal{H}_h := \mathcal{S}^1(\mathcal{T}) \times \mathcal{P}^0(\mathcal{E}_\Gamma)$. The bilinear form $\mathcal{B}_V : \mathcal{H}_h \times \mathcal{H}_h \to \mathbb{R}$ is given by

$$\mathcal{B}_V((w_h, \phi_h); (v_h, \psi_h)) := \mathcal{A}_V(w_h, v_h) - \langle \phi_h, \mathcal{I}_h^* v_h \rangle_\Gamma$$
$$+ \langle \psi_h, (1/2 - \mathcal{K}) w_h \rangle_\Gamma + \langle \psi_h, \mathcal{V} \phi_h \rangle_\Gamma,$$

and the linear functional $F_V : \mathcal{H}_h \to \mathbb{R}$ is given by

$$F_V((v_h, \psi_h)) := (f, \mathcal{I}_h^* v_h)_\Omega + \langle t_0, \mathcal{I}_h^* v_h \rangle_\Gamma + \langle \psi_h, (1/2 - \mathcal{K}) u_0 \rangle_\Gamma. \quad (26)$$

The (25a)–(25b) is equivalent to: find $\mathbf{u}_h \in \mathcal{H}_h$ such that

$$\mathcal{B}_V(\mathbf{u}_h; \mathbf{v}_h) = F_V(\mathbf{v}_h) \qquad \text{for all } \mathbf{v}_h \in \mathcal{H}_h. \quad (27)$$

3.3 Upwind scheme

In general it is a non trivial task to get a stable discrete solution for convection dominated problems. Finite volume schemes, however, allow an easy upwind stabilization [24]. If we want to apply an upwind scheme for the finite volume scheme, we replace $\mathbf{b} u_h$ on the interior dual edges/faces $V_i \setminus \Gamma$ in $\mathcal{A}_V$ (24) by an upwinded approximation. Given $V_i \in \mathcal{T}^*$, we consider the intersections with the neighboring cells $\tau_{ij} = V_i \cap V_j \neq \emptyset$ for $V_j \in \mathcal{T}^*$. Note that in two dimensions τ_{ij} is the union of two straight segments or (when the associated vertices $a_i, a_j \in \mathcal{N}$ lie on Γ) a single segment; see Fig. 1b. In three dimensions τ_{ij} consists of one or two polygonal surfaces. We then compute the averages

$$\beta_{ij} := \frac{1}{|\tau_{ij}|} \int_{\tau_{ij}} \mathbf{b} \cdot \mathbf{n}_i \, ds, \qquad \mathbf{A}_{ij} := \frac{1}{|\tau_{ij}|} \int_{\tau_{ij}} \mathbf{A} \, ds,$$

where $\mathbf{n}_i$ points outward with respect to V_i, and the parameter

$$\lambda_{ij} := \Phi(\beta_{ij} |\tau_{ij}| / \|\mathbf{A}_{ij}\|_\infty),$$

for a weight function $\Phi : \mathbb{R} \to [0, 1]$, which is being applied to the Péclet number. Then we consider the value

$$u_{h,ij} := \lambda_{ij} u_h(a_i) + (1 - \lambda_{ij}) u_h(a_j)$$

instead of u_h when restricted to $\tau_{ij} \subset \partial V_i \setminus \Gamma$. In this work we choose the upwind value defined by the classical (full) upwind scheme by

$$\Phi(t) := (\text{sign}(t) + 1)/2, \quad (28)$$

i.e., $\lambda_{ij} = 1$ for $\beta_{ij} \geq 0$ and $\lambda_{ij} = 0$ otherwise. A second choice will be

$$\Phi(t) := \begin{cases} \min\left\{2|t|^{-1}, 1\right\}/2 & \text{for } t < 0, \\ 1 - \min\left\{2|t|^{-1}, 1\right\}/2 & \text{for } t \geq 0, \end{cases} \quad (29)$$

where we can steer the amount of upwinding to reduce the excessive numerical diffusion. Whenever we apply an upwind scheme for the convection part, we replace the finite volume bilinear form $\mathcal{A}_V$ in the system (25a)–(25b) by

$$
\mathcal{A}_V^{up}(u_h, v_h) := \sum_{a_i \in \mathcal{N}} v_h(a_i) \left(\int_{\partial V_i \setminus \Gamma} -\mathbf{A}\nabla u_h \cdot \mathbf{n}\, ds + \int_{V_i} cu_h\, dx \right.
$$
$$
\left. + \sum_{j \in \mathcal{N}_i} \int_{\tau_{ij}} \mathbf{b} \cdot \mathbf{n}\, u_{h,ij}\, ds + \int_{\partial V_i \cap \Gamma^{out}} \mathbf{b} \cdot \mathbf{n}\, u_h\, ds \right),
$$
(30)

where $\mathcal{N}_i$ denotes the index set of nodes in $\mathcal{T}$ of all neighbors of $a_i \in \mathcal{N}$.

4 Stability and convergence

In this section we want to introduce a stabilized FVM–BEM coupling version of (27) for analysis purposes only. As in (14) we use the "implicit theoretical" stabilization of [1].

Similar as above we define $\widetilde{\mathcal{B}}_V : \mathcal{H}_h \times \mathcal{H}_h \to \mathbb{R}$ and $\widetilde{F}_V : \mathcal{H}_h \to \mathbb{R}$ by

$$
\widetilde{\mathcal{B}}_V(\mathbf{u}_h; \mathbf{v}_h) := \mathcal{B}_V(\mathbf{u}_h; \mathbf{v}_h) + \beta P(\mathbf{u}_h) P(\mathbf{v}_h), \tag{31}
$$
$$
\widetilde{F}_V(\mathbf{v}_h) := F_V(\mathbf{v}_h) + \beta \langle 1, (1/2 - \mathcal{K})u_0 \rangle_\Gamma P(\mathbf{v}_h). \tag{32}
$$

Then the stabilized FVM–BEM coupling reads: find $\mathbf{u}_h \in \mathcal{H}_h$, such that

$$
\widetilde{\mathcal{B}}_V(\mathbf{u}_h; \mathbf{v}_h) = \widetilde{F}_V(\mathbf{v}_h) \qquad \text{for all } \mathbf{v}_h \in \mathcal{H}_h. \tag{33}
$$

Remark 7 The discretized version of the stabilized FEM–BEM coupling reads with the stabilized weak form (14): find $\mathbf{u}_{h,FEM} \in \mathcal{H}_h$ such that

$$
\widetilde{\mathcal{B}}(\mathbf{u}_{h,FEM}; \mathbf{v}_h) = \widetilde{F}(\mathbf{v}_h) \qquad \text{for all } \mathbf{v}_h \in \mathcal{H}_h.
$$

See also Remark 4.

In the spirit of Lemma 2 and [1, Theorem 14] we can state the equivalence of the two presented FVM–BEM formulations.

Lemma 4 *The FVM–BEM coupling* (27) *and its stabilization* (33) *are equivalent. The statement is also true if we replace* $\mathcal{A}_V$ *by* $\mathcal{A}_V^{up}$ *in the corresponding bilinear forms.*

Proof In case of $\beta = 0$ the two formulations are obviously the same. Thus we only have to consider $\beta = 1$. If $\mathbf{u}_h = (u_h, \phi_h)$ is a solution of (27), testing with $\mathbf{v}_h = (0, 1)$ it follows that

$$
P(\mathbf{u}_h) = \langle 1, (1/2 - \mathcal{K})u_h + \mathcal{V}\phi_h \rangle_\Gamma = \langle 1, (1/2 - \mathcal{K})u_0 \rangle_\Gamma, \tag{34}
$$

which means that we can add the stabilization term to (27) to get the stabilized version (33). Reciprocally, testing (33) with $\mathbf{v}_h = (0, 1)$, it follows that

$$P(\mathbf{u}_h)(1 + \langle 1, \mathcal{V}1 \rangle_\Gamma) = \langle 1, (1/2 - \mathcal{K})u_0 \rangle_\Gamma (1 + \langle 1, \mathcal{V}1 \rangle_\Gamma).$$

Since the single layer operator is coercive, (34) follows and we can eliminate the β-dependent term in (33) to get (27). Note that the proof is independent of the particular choice of the finite volume bilinear form, and it therefore holds for $\mathcal{A}_V^{up}$ as well. $\qquad\square$

The idea of our analysis is to estimate the difference of the stabilized FEM–BEM coupling and the stabilized FVM–BEM coupling. For that we need the following two estimates, which are standard in the context of FVM [5,11,15] with the above constructed dual mesh, but here extended to the coupling problem.

Lemma 5 *For the difference of the right-hand side of* (9) *and* (26)*, there holds*

$$|F(\mathbf{v}_h) - F_V(\mathbf{v}_h)| \leq C \left(\sum_{T \in \mathcal{T}} h_T \|f\|_{L^2(T)} \|\nabla v_h\|_{L^2(T)} \right.$$
$$\left. + \sum_{E \in \mathcal{E}_\Gamma} h_E^{1/2} \|t_0 - \bar{t}_0\|_{L^2(E)} \|\nabla v_h\|_{L^2(T_E)} \right) \quad (35)$$

for all $\mathbf{v}_h = (v_h, \psi_h) \in \mathcal{H}_h$ *with a constant* $C > 0$*, which depends only on the shape regularity constant. Here,* $\bar{t}_0$ *is the* $\mathcal{E}_\Gamma$*-piecewise integral mean of* t_0 *and* T_E *is the element associated with* E*.*

Proof It is easy to see that from (9) and (26) we get

$$|F(\mathbf{v}_h) - F_V(\mathbf{v}_h)| = |(f, v_h - \mathcal{I}_h^* v_h)_\Omega + \langle t_0, v_h - \mathcal{I}_h^* v_h \rangle_\Gamma|.$$

The triangle inequality and the Cauchy–Schwarz inequality and (20)–(22) lead to the assertion. $\qquad\square$

The next lemma gives us an estimate between the weak and the finite volume bilinear form for a function $v_h \in \mathcal{S}^1(\mathcal{T})$.

Lemma 6 *Let us assume that* $\mathbf{b} \cdot \mathbf{n}$ *is piecewise constant on* Γ^{in}*, i.e.,* $\mathbf{b} \cdot \mathbf{n}|_{\Gamma^{in}} \in \mathcal{P}^0(\mathcal{E}_\Gamma^{in})$*. For all* $v_h, w_h \in \mathcal{S}^1(\mathcal{T})$ *there hold*

$$|\mathcal{A}(w_h, v_h) - \mathcal{A}_V(w_h, v_h)| \leq C_1 \sum_{T \in \mathcal{T}} \left(h_T \|w_h\|_{H^1(T)} \|v_h\|_{H^1(T)} \right), \quad (36)$$

$$|\mathcal{A}(w_h, v_h) - \mathcal{A}_V^{up}(w_h, v_h)| \leq C_2 \sum_{T \in \mathcal{T}} \left(h_T \|w_h\|_{H^1(T)} \|v_h\|_{H^1(T)} \right), \quad (37)$$

with constants $C_1, C_2 > 0$*, depending only on the model data* $\mathbf{A}$*,* $\mathbf{b}$*,* c*, and on the shape regularity constant.*

Proof Let us define $v_h^* := \mathcal{I}_h^* v_h \in \mathcal{P}^0(\mathcal{T}^*)$. Using integration by parts for $\mathcal{A}(w_h, v_h)$ and $\mathcal{A}_V(w_h, v_h)$ the lines in the proof of [11, Lemma 5.2] show with (20)

$$
\mathcal{A}(w_h, v_h) - \mathcal{A}_V(w_h, v_h)
$$

$$
= \sum_{T \in \mathcal{T}} \Bigg((-(\operatorname{div} \mathbf{A})\nabla w_h + (\operatorname{div} \mathbf{b})w_h + \mathbf{b} \cdot \nabla w_h + cw_h, v_h - v_h^*)_T
$$

$$
+ \sum_{E \in \mathcal{E}_T} ((\mathbf{A} - \overline{\mathbf{A}})\nabla w_h \cdot \mathbf{n}, v_h - v_h^*)_E
$$

$$
- \sum_{E \in \mathcal{E}_T \cap \Gamma^{in}} (\mathbf{b} \cdot \mathbf{n}(w_h - \overline{w}_h), v_h - v_h^*)_E \Bigg). \tag{38}
$$

Here, $\operatorname{div} \mathbf{A}$ is the divergence operator applied to the columns of $\mathbf{A}$, $\overline{\mathbf{A}} = (1/|T|) \int_T \mathbf{A}\, dx$, i.e., [11, Lemma 5.2] applies also for the piecewise integral means of the entries in $\mathbf{A}$ on T, and $\overline{w}_h \in \mathcal{P}^0(\mathcal{E}_\Gamma)$ is the best $L^2(\Gamma)$ approximation of w_h. With the fact that ∇w_h as well as the outer normal vector $\mathbf{n}$ of T are constant on E, we prove with standard approximation arguments

$$
|\mathcal{A}(w_h, v_h) - \mathcal{A}_V(w_h, v_h)| \le \sum_{T \in \mathcal{T}} C_T \Bigg(\|w_h\|_{H^1(T)} \|v_h - v_h^*\|_{L^2(T)}
$$

$$
+ \sum_{E \in \mathcal{E}_T} \|\mathbf{A} - \overline{\mathbf{A}}\|_{L^\infty(T)} \|\nabla w_h\|_{L^2(E)} \|v_h - v_h^*\|_{L^2(E)}
$$

$$
+ \sum_{E \in \mathcal{E}_T \cap \mathcal{E}_\Gamma^{in}} \|w_h - \overline{w}_h\|_{L^2(E)} \|v_h - v_h^*\|_{L^2(E)} \Bigg).
$$

Here, the constant $C_T > 0$ only depends on the shape regularity constant, and the model data $\mathbf{A}$, $\mathbf{b}$, and c. Next we note that there holds $\|\mathbf{A} - \overline{\mathbf{A}}\|_{L^\infty(T)} \le Ch_T \|\mathbf{A}\|_{W^{1,\infty}(T)}$, i.e., the Poincaré inequality in $W^{1,\infty}(T)$ applies because of the uniform continuity of $\mathbf{A}|_T$; see [14, proof for equation (34)]. Together with the standard scaling inequalities $\|\nabla w_h\|_{L^2(E)} \le Ch_E^{-1/2} \|\nabla w_h\|_{L^2(T)}$ and $\|w_h - \overline{w}_h\|_{L^2(E)} \le Ch_T^{1/2} \|\nabla w_h\|_{L^2(T)}$, (21)–(22), we prove (36). To prove (37) we write

$$
|\mathcal{A}(w_h, v_h) - \mathcal{A}_V^{up}(w_h, v_h)| \le |\mathcal{A}(w_h, v_h) - \mathcal{A}_V(w_h, v_h)|
$$

$$
+ |\mathcal{A}_V(w_h, v_h) - \mathcal{A}_V^{up}(w_h, v_h)|.
$$

Note that we can directly apply (36) for the first and [11, Lemma 6.1] for the second difference to show (37). □

Remark 8 If $\mathbf{A}$ is $\mathcal{T}$-piecewise constant, all parts with $\mathbf{A}$ vanish in (38) because of $\operatorname{div} \mathbf{A} = 0$ and (20) since ∇w_h is constant. This is well-known and if $\mathbf{b} = (0, 0)^T$ and $c = 0$ there even holds $\mathcal{A}(w_h, v_h) = \mathcal{A}_V(w_h, v_h)$, see, e.g., [2,18].

Collecting all the results together we prove:

Lemma 7 *Let us assume that* $\mathbf{b}\cdot\mathbf{n}$ *is piecewise constant on* Γ^{in}, *i.e.*, $\mathbf{b}\cdot\mathbf{n}|_{\Gamma^{in}} \in \mathcal{P}^0(\mathcal{E}_\Gamma^{in})$. *For all* $\mathbf{w}_h = (w_h, \xi_h) \in \mathcal{H}_h$ *and* $\mathbf{v}_h = (v_h, \psi_h) \in \mathcal{H}_h$ *there holds*

$$|\widetilde{\mathcal{B}}(\mathbf{w}_h; \mathbf{v}_h) - \widetilde{\mathcal{B}}_V(\mathbf{w}_h; \mathbf{v}_h)| \leq C \sum_{T \in \mathcal{T}} \left(h_T \|w_h\|_{H^1(T)} \|v_h\|_{H^1(T)}\right) \qquad (39)$$

with a constant $C > 0$, *which depends only on the model data* **A**, **b**, c, *and the shape regularity constant. The statement is also true if we replace* $\mathcal{A}_V$ *by* $\mathcal{A}_V^{up}$ *in the corresponding bilinear forms.*

Proof We estimate

$$|\widetilde{\mathcal{B}}(\mathbf{w}_h; \mathbf{v}_h) - \widetilde{\mathcal{B}}_V(\mathbf{w}_h; \mathbf{v}_h)| = |\mathcal{A}(w_h, v_h) - \mathcal{A}_V(w_h, v_h) - \langle \xi_h, v_h - \mathcal{I}_h^* v_h \rangle_\Gamma|$$

$$\leq C \sum_{T \in \mathcal{T}} \left(h_T \|w_h\|_{H^1(T)} \|v_h\|_{H^1(T)}\right),$$

where we used (36) and (20) since $\xi_h \in \mathcal{P}^0(\mathcal{E}_\Gamma)$. Using (37), the proof with $\mathcal{A}_V^{up}$ follows from this bound. $\qquad\square$

Theorem 2 (Stability) *There exists* $H > 0$ *such that the following statement is valid provided that* $\mathcal{T}$ *is sufficiently fine, i.e.,* $h := \max_{T \in \mathcal{T}} h_T < H$: *Let* $\lambda_{\min}(\mathbf{A}) > C_\mathcal{K}/4$ *with the contraction constant* $C_\mathcal{K} \in [1/2, 1)$ *of the double layer potential. Furthermore, let* $\mathbf{b}\cdot\mathbf{n}$ *be piecewise constant on* Γ^{in}, *i.e.*, $\mathbf{b}\cdot\mathbf{n}|_{\Gamma^{in}} \in \mathcal{P}^0(\mathcal{E}_\Gamma^{in})$. *Then, there exists a constant* $C_{\text{Vstab}} > 0$ *such that*

$$\widetilde{\mathcal{B}}_V(\mathbf{v}_h; \mathbf{v}_h) \geq C_{\text{Vstab}} \|\mathbf{v}_h\|_\mathcal{H}^2 \quad \text{for all } \mathbf{v}_h \in \mathcal{H}_h. \qquad (40)$$

The constant $C_{\text{Vstab}} > 0$ *depends only on the model data* **A**, **b**, c, *the contraction constant* $C_\mathcal{K}$, *and the shape regularity constant. In particular, existence and uniqueness of the discrete solution* $\mathbf{u}_h = (u_h, \phi_h) \in \mathcal{H}_h = \mathcal{S}^1(\mathcal{T}) \times \mathcal{P}^0(\mathcal{E}_\Gamma))$ *of our FVM–BEM coupling* (27) *follow directly from Lemma* 4. *The statement also holds if we replace* $\mathcal{A}_V$ *by* $\mathcal{A}_V^{up}$ *in the corresponding bilinear forms.*

Proof From (39) we see with $C' > 0$

$$\widetilde{\mathcal{B}}_V(\mathbf{v}_h; \mathbf{v}_h) \geq \widetilde{\mathcal{B}}(\mathbf{v}_h; \mathbf{v}_h) - C'h\|v_h\|_{H^1(\Omega)}^2.$$

The stability estimate (17) provides $\widetilde{\mathcal{B}}(\mathbf{v}_h; \mathbf{v}_h) \geq C_{\text{stab}}'\|\mathbf{v}_h\|_\mathcal{H}^2$ with $C_{\text{stab}}' > 0$, which proves the coercivity estimate for h small enough. The proof with $\mathcal{A}_V^{up}$ is the same. $\square$

Theorem 3 (A priori convergence estimate) *There exists* $H > 0$ *such that the following statement is valid provided that* $\mathcal{T}$ *is sufficiently fine, i.e.,* $h := \max_{T \in \mathcal{T}} h_T < H$: *Let* $\lambda_{\min}(\mathbf{A}) > C_\mathcal{K}/4$ *with the contraction constant* $C_\mathcal{K} \in [1/2, 1)$ *of the double layer potential* $\mathcal{K}$. *Furthermore, let* $\mathbf{b}\cdot\mathbf{n}$ *be piecewise constant on* Γ^{in}, *i.e.*, $\mathbf{b}\cdot\mathbf{n}|_{\Gamma^{in}} \in \mathcal{P}^0(\mathcal{E}_\Gamma^{in})$. *For the solution* $\mathbf{u} = (u, \phi) \in \mathcal{H} = H^1(\Omega) \times H^{-1/2}(\Gamma)$ *of our model problem* (10)

and the discrete solution $\mathbf{u}_h = (u_h, \phi_h) \in \mathcal{H}_h = \mathcal{S}^1(\mathcal{T}) \times \mathcal{P}^0(\mathcal{E}_\Gamma))$ *of our FVM–BEM coupling* (27) *there holds*

$$\|\mathbf{u} - \mathbf{u}_h\|_{\mathcal{H}}$$
$$\leq C_{\text{est}} \left(h\|f\|_{L^2(\Omega)} + h^{1/2}\|t_0 - \bar{t}_0\|_{L^2(\Gamma)} + (1 + h) \inf_{\mathbf{v}_h \in \mathcal{H}_h} \|\mathbf{u} - \mathbf{v}_h\|_{\mathcal{H}} + h\|\mathbf{u}\|_{\mathcal{H}} \right),$$

where $\bar{t}_0$ *is the* $\mathcal{E}_\Gamma$-*piecewise integral mean of* t_0. *The constant* $C_{\text{est}} > 0$ *depends only on the model data* **A**, **b**, c, *the contraction constant* $C_\mathcal{K}$, *and the shape regularity constant. In particular, if* $u \in H^2(\Omega)$, $\phi \in H^{1/2}(\mathcal{E}_\Gamma)$, *and* $t_0 \in H^{1/2}(\mathcal{E}_\Gamma)$, *where*

$$H^{1/2}(\mathcal{E}_\Gamma) := \left\{ v \in L^2(\Gamma) \,\middle|\, v|_E \in H^{1/2}(E) \ \text{for all} \ E \in \mathcal{E}_\Gamma \right\},$$

we have first order convergence

$$\|\mathbf{u} - \mathbf{u}_h\|_{\mathcal{H}} = \mathcal{O}(h).$$

The statement is also true if we replace $\mathcal{A}_V$ *by* $\mathcal{A}_V^{up}$ *in the corresponding bilinear forms.*

In the following proof of Theorem 3, we write the symbol $\lesssim$, if an estimate holds up to a multiplicative constant, which depends only on the model data **A**, **b**, c, the contraction constant $C_\mathcal{K}$, and the shape regularity constant.

Proof For arbitrary $\mathbf{v}_h = (v_h, \psi_h) \in \mathcal{H}_h$ we define $\mathbf{w}_h = (w_h, \varphi_h) := \mathbf{u}_h - \mathbf{v}_h \in \mathcal{H}_h$. Then we get with (40)

$$\|\mathbf{u}_h - \mathbf{v}_h\|_{\mathcal{H}}^2 \lesssim \widetilde{\mathcal{B}}_V(\mathbf{u}_h; \mathbf{w}_h) - \widetilde{\mathcal{B}}_V(\mathbf{v}_h; \mathbf{w}_h)$$
$$= \widetilde{F}_V(\mathbf{w}_h) - \widetilde{F}(\mathbf{w}_h) + \widetilde{\mathcal{B}}(\mathbf{u}; \mathbf{w}_h) - \widetilde{\mathcal{B}}_V(\mathbf{v}_h; \mathbf{w}_h),$$

where we used the finite volume discrete system (33) and the FEM–BEM bilinear from (14) with discrete test functions $\mathbf{w}_h \in \mathcal{H}_h$. We remind that the solution of (10) and the discrete solution of (27) are equivalent to the solutions of (14) and (33), respectively; see Lemma 2 and Lemma 4. Since $\widetilde{F}_V(\mathbf{w}_h) - \widetilde{F}(\mathbf{w}_h) = F_V(\mathbf{w}_h) - F(\mathbf{w}_h)$ we apply (35) and insert $\mathbf{v}_h$ to estimate

$$\|\mathbf{u}_h - \mathbf{v}_h\|_{\mathcal{H}}^2 \lesssim h\|f\|_{L^2(\Omega)}\|\nabla w_h\|_{L^2(\Omega)} + h_{\mathcal{E}_\Gamma}^{1/2}\|t_0 - \bar{t}_0\|_{L^2(\Gamma)}\|\nabla w_h\|_{L^2(\Omega)}$$
$$+ \widetilde{\mathcal{B}}(\mathbf{u} - \mathbf{v}_h; \mathbf{w}_h) + \widetilde{\mathcal{B}}(\mathbf{v}_h; \mathbf{w}_h) - \widetilde{\mathcal{B}}_V(\mathbf{v}_h; \mathbf{w}_h),$$

where $h_{\mathcal{E}_\Gamma} := \max_{E \in \mathcal{E}_\Gamma} h_E$. For the third to last term on the right-hand side we apply the boundedness of $\widetilde{\mathcal{B}}$ and we estimate the last two terms with (39). Thus we obtain

$$\|\mathbf{u}_h - \mathbf{v}_h\|_{\mathcal{H}}^2 \lesssim h\|f\|_{L^2(\Omega)}\|\nabla w_h\|_{L^2(\Omega)} + h_{\mathcal{E}_\Gamma}^{1/2}\|t_0 - \bar{t}_0\|_{L^2(\Gamma)}\|\nabla w_h\|_{L^2(\Omega)}$$
$$+ \|\mathbf{u} - \mathbf{v}_h\|_{\mathcal{H}}\|\mathbf{w}_h\|_{\mathcal{H}} + h\|v_h\|_{H^1(\Omega)}\|w_h\|_{H^1(\Omega)}.$$

Finally with $\|w_h\|_{H^1(\Omega)} \leq \|\mathbf{w}_h\|_{\mathcal{H}} = \|\mathbf{u}_h - \mathbf{v}_h\|_{\mathcal{H}}$ we get

$$\|\mathbf{u}_h - \mathbf{v}_h\|_{\mathcal{H}} \lesssim h\|f\|_{L^2(\Omega)} + h_{\mathcal{E}_\Gamma}^{1/2}\|t_0 - \bar{t}_0\|_{L^2(\Gamma)} + \|\mathbf{u} - \mathbf{v}_h\|_{\mathcal{H}} + h\|v_h\|_{H^1(\Omega)}.$$

With $\|v_h\|_{H^1(\Omega)} \leq \|\mathbf{u} - \mathbf{v}_h\|_{\mathcal{H}} + \|\mathbf{u}\|_{\mathcal{H}}$ and

$$\|\mathbf{u} - \mathbf{u}_h\|_{\mathcal{H}} \leq \|\mathbf{u} - \mathbf{v}_h\|_{\mathcal{H}} + \|\mathbf{u}_h - \mathbf{v}_h\|_{\mathcal{H}}$$

we get the assertion with $h_{\mathcal{E}_\Gamma} \geq h$. The proof with $\mathcal{A}_V^{up}$ is the same. $\qquad\square$

Remark 9 In [11, see Remark 5.1], where we consider a FVM–BEM coupling with a three field coupling approach, we have the constraint $\phi \in L^2(\Gamma)$ in the case $\gamma(x) = 0$ from assumption (2) to get convergence and an error estimate. Note that this regularity is not needed therein to prove existence and uniqueness, see [11, see Remark 5.2]. Furthermore, there is also an additional assumption necessary in the case $\gamma(x) = 0$, namely div $\mathbf{b} + c = 0$ in Ω and $\mathbf{b} \cdot \mathbf{n} = 0$ on Γ^{in}. Thus Theorem 2, which essentially shows existence and uniqueness of a discrete solution, and Theorem 3 for our non-symmetric FVM–BEM coupling are much stronger than what is available for the three field FVM–BEM coupling. However, the constraint $\lambda_{\min}(\mathbf{A}) > C_{\mathcal{K}}/4$ on the eigenvalues of $\mathbf{A}$ is not needed for the three field FVM–BEM coupling.

5 Numerical results

In this section we verify our new coupling with three examples in two dimensions. We stress that in all experiments we consider the discrete FVM–BEM system (25a)–(25b) and (27), respectively, where we replace $\mathcal{A}_V$ defined in (24) by the upwind form $\mathcal{A}_V^{up}$ defined in (30) if we use an upwind scheme for the convection part. We mention once again, that the equivalent stabilized FVM–BEM system (33) is only needed for theoretical reasons.

All the numerical experiments are done in MATLAB on a standard laptop with a dual core 2.8 GHz processor and 16 GB memory. Only the implementation of the matrices resulting from the $\mathcal{V}$ and $\mathcal{K}$ expressions is done in C using the *mex*-interface of MATLAB [11,12]. As introduced earlier, we use the equivalence of norms, i.e., $\|\phi - \phi_h\|_{H^{-1/2}(\Gamma)}^2 \sim \|\phi - \phi_h\|_{\mathcal{V}}^2 := \langle \mathcal{V}(\phi - \phi_h), \phi - \phi_h \rangle_\Gamma$, to calculate the conormal error $\phi - \phi_h$. Then $\|\phi - \phi_h\|_{\mathcal{V}}$ leads to an approximation of a double integral by quadrature. The details can be found in [10–12]. In all experiments and in each iteration, $\mathcal{T}$ consists of triangles, which are up to rotation congruent. In this work we only consider uniform mesh refinement, i.e., we divide all triangles by four triangles.

5.1 Mexican hat problem

We consider the square $\Omega = (-1/4, 1/4)^2$. We take the exact solution to be $u(x_1, x_2) = (1 - 100x_1^2 - 100x_2^2)e^{-50(x_1^2 + x_2^2)}$ in the interior domain Ω and $u_e(x_1, x_2) =$
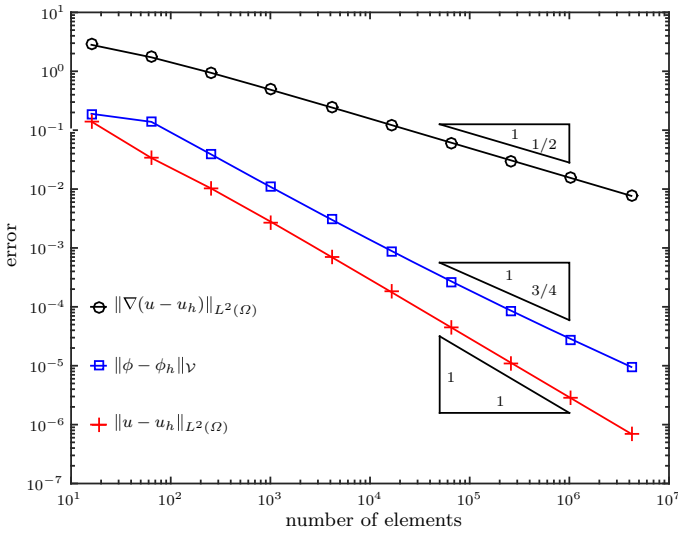
Fig. 2 The error $\|\nabla(u - u_h)\|_{L^2(\Omega)}$ in the H^1 semi-norm, the error $\|u - u_h\|_{L^2(\Omega)}$ in the L^2 norm, and the conormal error $\|\phi - \phi_h\|_{\mathcal{V}}$ in the $\mathcal{V}$ norm in the example in Sect. 5.1 for uniform mesh-refinement
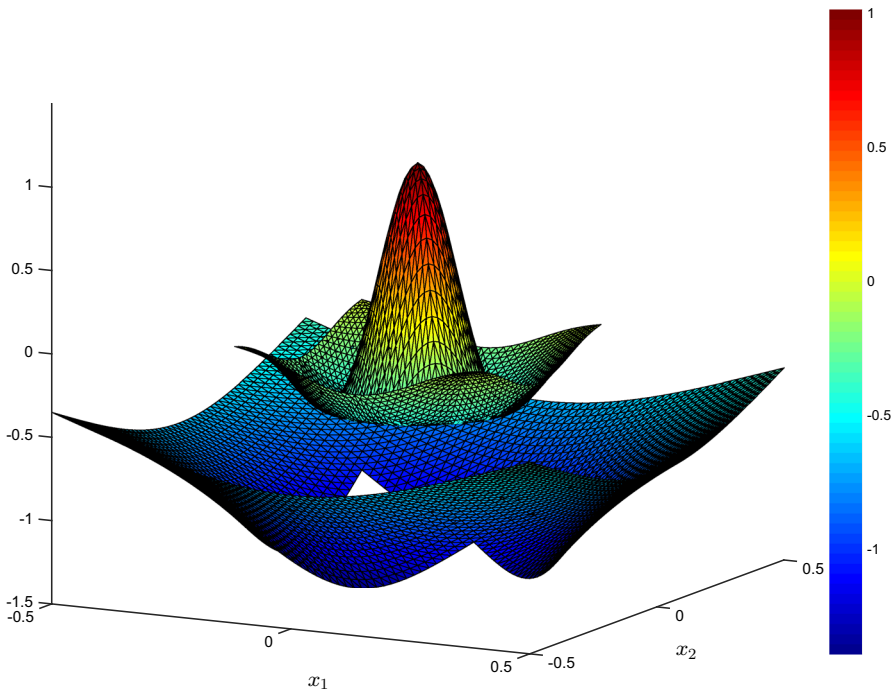

Fig. 3 Interior and exterior solution on an uniformly generated mesh with 4096 elements in the example in Sect. 5.1

$\log \sqrt{x_1^2 + x_2^2}$ in the exterior domain Ω_e. The diffusion matrix is

$$\mathbf{A} = \begin{pmatrix} 10 + \cos x_1 & 160\, x_1 x_2 \\ 160\, x_1 x_2 & 10 + \sin x_2 \end{pmatrix}, \tag{41}$$

and we take $\mathbf{b} = (0, 0)^T$ and $c = 0$. Note that in Ω we have $\lambda_{\min}(\mathbf{A}) = 0.342278$ and $\lambda_{\max}(\mathbf{A}) = 10.247271$. The right-hand side f and the jumps u_0 and t_0 are calculated appropriately. We stress that u and u_e are smooth in Ω and Ω_e, respectively. Therefore, we expect a convergence order $\mathcal{O}(h^1)$ for a first order numerical scheme in the H^1 norm, where $h := \max_{T \in \mathcal{T}} h_T$ denotes the uniform mesh-size. This corresponds to order $\mathcal{O}(N^{-1/2})$ with respect to the number of elements N of $\mathcal{T}$. The initial mesh $\mathcal{T}^{(0)}$ consists of 16 triangles. Figure 2 shows the curves of the interior error $u - u_h$ in the H^1 semi-norm and L^2 norm, respectively, and the conormal error of $\phi - \phi_h$ in the $\mathcal{V}$ norm. Both axes are scaled logarithmically; i.e., a straight line g with slope $-p$ corresponds to a dependence $g = \mathcal{O}(N^{-p}) = \mathcal{O}(h^{2p})$. The interior H^1 semi-norm error leads to a convergence order $\mathcal{O}(N^{-1/2})$, whereas the corresponding L^2 norm error decreases with $\mathcal{O}(N^{-1})$. Thus, the error in H^1 norm behaves like $\mathcal{O}(N^{-1/2})$. The convergence of the BEM conormal quantity is optimal in the sense of $\mathcal{O}(N^{-3/4})$ due to the smooth solution. Altogether we see $\|\mathbf{u} - \mathbf{u}_h\|_{\mathcal{H}} = \mathcal{O}(N^{-1/2}) = \mathcal{O}(h)$ with $\mathbf{u} = (u, \phi)$ and $\mathbf{u}_h = (u_h, \phi_h) \in \mathcal{H}_h$, which was shown in Theorem 3 for smooth solutions.

Figure 3 shows the solution in Ω and parts of Ω_e. We observe the jump on the coupling boundary Γ and remark that the BEM solution is generated pointwise with the aid of the exterior representation formula (3) on a uniform grid. For points on the boundary Γ coming from the exterior domain, we use the exterior trace of (3). Note that instead of (4) this approximated trace reads

$$u_{e,h}|_\Gamma(x) = -(\mathcal{V}\phi_h)(x) + \left(\left(\mathcal{K} + \frac{\varphi}{2\pi}\right)(u_h - u_0)\right)(x) \tag{42}$$

for a point evaluation $x \in \Gamma$, where φ is the interior angle of the intersection of the two tangential vectors in x.

Remark 10 For this example $\gamma(x) = 0$ from assumption (2). Thus the analysis needs the stabilized bilinear form (31) with $\beta = 1$ from (11). We also remind that, we have the condition $\lambda_{\min}(\mathbf{A}) > C_{\mathcal{K}}/4$, where $C_{\mathcal{K}} \in [1/2, 1)$ is the contraction constant of the double layer potential $\mathcal{K}$, for our analysis. Note that our $\mathbf{A}$ with $\lambda_{\min}(\mathbf{A}) = 0.342278$ fulfills this constraint. If one replace both values of 160 by 165 we get $\lambda_{\min}(\mathbf{A}) = 0.003033$ which contradicts the bound. However, the experiments (not plotted here) show the right convergence behavior. This confirms similar observations for FEM–BEM couplings, e.g., [1]. In particular, the bound seems to be a theoretical bound also for our FVM–BEM coupling approach.

5.2 Convection–diffusion problem

We consider the model problem on the square domain $\Omega = (0, 1/2) \times (0, 1/2)$. We choose a fixed diffusion matrix of $\mathbf{A} = 0.5\,\mathbf{I}$, a convection field $\mathbf{b} = (1000 x_1, 0)^T$
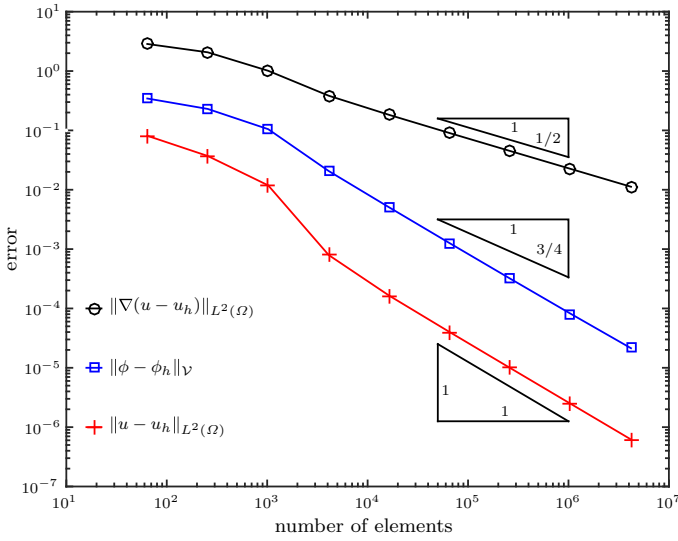
Fig. 4 The error $\|\nabla(u - u_h)\|_{L^2(\Omega)}$ in the H^1 semi-norm, the error $\|u - u_h\|_{L^2(\Omega)}$ in the L^2 norm, and the conormal error $\|\phi - \phi_h\|_{\mathcal{V}}$ in the $\mathcal{V}$ norm in the example in Sect. 5.2 for uniform mesh-refinement
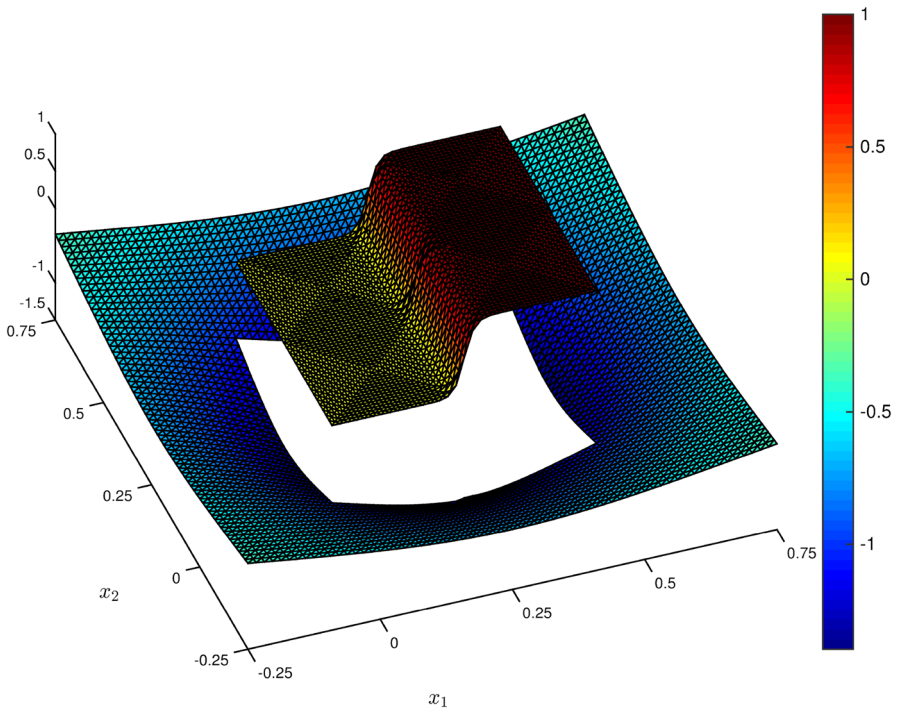

Fig. 5 Interior and exterior solution with a weighted upwinding stabilization on an uniformly generated mesh with 4096 elements in the example in Sect. 5.2

and a reaction coefficient $c = 0$. Note that for this problem we do not have an inflow boundary Γ^{in} and thus (1f) is not needed. For all calculations we use the upwind discrete coupling with the weighting function Φ defined in (29). We prescribe an analytical solution

$$u(x_1, x_2) = 0.5 \left(1 - \tanh \left(\frac{0.25 - x_1}{0.02} \right) \right)$$

for the interior domain Ω and

$$u_e(x_1, x_2) = \log \sqrt{(x_1 - 0.25)^2 + (x_2 - 0.25)^2}$$

for the exterior domain Ω_e. We calculate the right-hand side f and the jumps u_0 and t_0 appropriately. Note that $\lambda_{\min}(\mathbf{A}) = 0.5$ and that the problem is highly convection dominated.

The initial mesh $\mathcal{T}^{(0)}$ consists of 64 triangles. In Fig. 4 we plot the convergence rate for uniform mesh-refinement with respect to the number of elements N in $\mathcal{T}$. Since the interior and exterior solution are smooth as in the previous example in Sect. 5.1, we observe a similar convergence behavior, in particular, $\|\mathbf{u} - \mathbf{u}_h\|_{\mathcal{H}} = \mathcal{O}(N^{-1/2}) = \mathcal{O}(h)$ with $\mathbf{u} = (u, \phi)$ and $\mathbf{u}_h = (u_h, \phi_h) \in \mathcal{H}_h$, which also confirms Theorem 3. However, due to the strong convection, we have a preasymptotic phase. We want to mention that without any upwind stabilization, it is not possible to get a stable solution even for more than 4 million elements, which is the last mesh in our calculation. In Fig. 5 we plot the interior and exterior solution. To resolve the shock at $x_1 = 0.25$ better and thus to reduce the effects to the exterior domain, one can use adaptive mesh refinement as in [13]. However, this is beyond this work.

5.3 A more practical example

Our last example is a more practical problem. The model can describe the stationary concentration of a chemical dissolved and distributed in different fluids, where we have a convection dominated problem in Ω and a diffusion distribution in Ω_e. Note that the interior is a classical model problem and as described above, the coupling with the exterior problem can "replace" the boundary condition, which might be difficult to find. Our interior domain $\Omega = (-1/4, 1/4)^2 \backslash ([0, 1/4] \times [-1/4, 0])$ is the classical L-shape. The diffusion matrix $\mathbf{A} = \alpha \mathbf{I}$ in Ω is piecewise constant and reads

$$\alpha : \mathbb{R} \times \mathbb{R} \to \mathbb{R} : (x_1, x_2) \mapsto \begin{cases} 10^{-7} & \text{for } x_2 \leq 0, \\ 10^{-6} & \text{for } x_1 > 0, \\ 5 \cdot 10^{-7} & \text{else.} \end{cases}$$

Additionally, we choose $\mathbf{b} = (15, 10)^T$ and $c = 10^{-2}$. The source is in the lower square, i.e., $f = 5$ for $-0.2 \leq x_1 \leq -0.1$, $-0.2 \leq x_2 \leq -0.05$, and $f = 0$ elsewhere. We prescribe the jumps $u_0 = 0$ and $t_0 = 0$. Instead of a logarithmic radiation condition, we impose that $u = a_\infty + \mathcal{O}(1/|x|)$ and $|x| \to \infty$ for an unknown

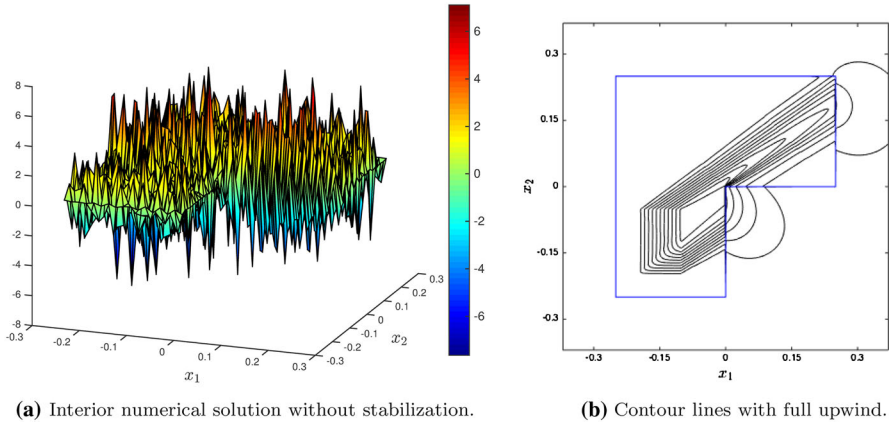**(a)** Interior numerical solution without stabilization.   **(b)** Contour lines with full upwind.

Fig. 6 A convection approximation without upwinding or any other stabilization leads to strong oscillations in (**a**) in the example in Sect. 5.3. In (**b**) we see the transmission effects of the interior and exterior problem through a contour line *plot*

$a_\infty \in \mathbb{R}$. An exterior solution of the Laplace equation satisfying this type of asymptotic behavior at infinity must have zero average of the normal derivative on Γ, see [9]. We must add a_∞ to the representation formulas for the exterior solution (3) and (42), respectively, and (4) becomes

$$u_e|_\Gamma = (1/2 + \mathcal{K})u_e|_\Gamma - \mathcal{V}\phi + a_\infty.$$

Thus we have an additional term $\langle \psi_h, a_\infty \rangle_\Gamma$ on the left-hand side of (25b) and an additional equation, which ensures $\langle 1, \phi_h \rangle_\Gamma = 0$, as the counterpart. We use the full upwind scheme, i.e., (28), for the approximation of the convection term and start with a mesh of 48 triangles. This example is similar to the one in [11, Subsection 7.2] but with a smaller diffusion. Note that the problem is highly convection dominated and the analytical solution is unknown. An interior solution without any stabilization is plotted in Fig. 6a and shows strong oscillations. In Fig. 6b we see the contour lines based on a solution generated on a mesh $\mathcal{T}$ with 49,152 elements. The transport is mainly from the source $f \neq 0$ in the left lower square in the direction of the convection **b**. We also can see the interaction with the exterior domain, hence, the contour lines are circular. In general, the solution of such a problem may have local phenomena such as injection wells. As seen in Fig. 7 this leads to step layers on the boundary $(0, 0)$ to $(0, -1/4)$, due to the convection in this direction and the different diffusion coefficient of the interior and exterior problem. Since we consider here a domain with a reentrant corner and model data with jumps, it is well known that uniform mesh refinement can not guarantee optimal convergence rates, i.e., $u \notin H^2(\Omega)$. An adaptive mesh refinement steered through a robust a posteriori estimator could lead to a more accurate solution as one can find in a similar example for the FVM–BEM three field coupling approach in [13].
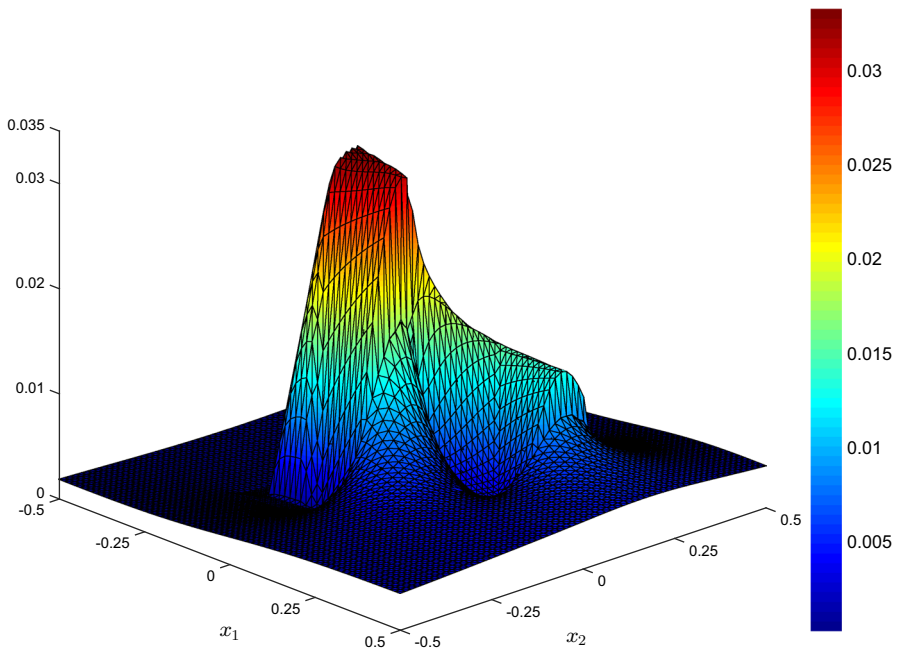
Fig. 7 Interior and exterior solution with full upwinding stabilization on an uniformly generated mesh with 3072 elements in the example in Sect. 5.3

6 Conclusions

We presented a new FVM–BEM coupling method based on the non-symmetric approach to solve a transmission problem, i.e., a convection diffusion reaction problem in an interior domain coupled with a diffusion process in an unbounded exterior domain. The resulting scheme maintains local flux conservation, also in the case when an upwind scheme for convection dominated problems is used. We showed ellipticity of the continuous and discrete system or for some model configurations the ellipticity of their equivalent stabilized system. Additionally, we could improve the theoretical elliptic constant from previous works. Note that the stabilized FVM–BEM system was only used for theoretical purposes. This allowed us to show existence and uniqueness, convergence, and an a priori estimate. We stress that for some critical model configurations the assumptions on the data and regularity of the unknown solution are weaker than for the comparable three field FVM–BEM coupling. Moreover, the non-symmetric approach has less discrete unknowns and thus is computational cheaper. Our work gives us a recipe for the coupling of BEM with a non-Galerkin method like FVM. Our theoretical results were confirmed by three numerical examples, which illustrate the strength of the chosen method in terms of local flux conservation and convection dominated problems.

References

1. Aurada, M., Feischl, M., Führer, T., Karkulik, M., Melenk, J.M., Praetorius, D.: Classical FEM–BEM coupling methods: nonlinearities, well-posedness, and adaptivity. Comput. Mech. **51**(4), 399–419 (2013)
2. Bank, R.E., Rose, D.J.: Some error estimates for the box method. SIAM J. Numer. Anal. **24**(4), 777–787 (1987)
3. Brezzi, F., Johnson, C.: On the coupling of boundary integral and finite element methods. Calcolo **16**(2), 189–201 (1979)
4. Cai, Z.: On the finite volume element method. Numer. Math. **58**(7), 713–735 (1991)
5. Chatzipantelidis, P.: Finite volume methods for elliptic PDE's: a new approach. M2AN. Math. Model. Numer. Anal. **36**(2), 307–324 (2002)
6. Ciarlet, P.G.: The Finite Element Method for Elliptic Problems. North-Holland, Amsterdam (1978)
7. Costabel, M.: Symmetric methods for the coupling of finite elements and boundary elements. In: Boundary Elements IX, vol. 1 (Stuttgart, 1987), pp. 411–420. Comput. Mech., Southampton (1987)
8. Costabel, M.: Boundary integral operators on Lipschitz domains: elementary results. SIAM J. Math. Anal. **19**(3), 613–626 (1988)
9. Costabel, M., Stephan, E.P.: A direct boundary integral equation method for transmission problems. J. Math. Anal. Appl. **106**(2), 367–413 (1985)
10. Erath, C.: Coupling of the Finite Volume Method and the Boundary Element Method—Theory, Analysis, and Numerics. Ph.D. thesis, University of Ulm (2010)
11. Erath, C.: Coupling of the finite volume element method and the boundary element method: an a priori convergence result. SIAM J. Numer. Anal. **50**(2), 574–594 (2012)
12. Erath, C.: A new conservative numerical scheme for flow problems on unstructured grids and unbounded domains. J. Comput. Phys. **245**, 476–492 (2013)
13. Erath, C.: A posteriori error estimates and adaptive mesh refinement for the coupling of the finite volume method and the boundary element method. SIAM J. Numer. Anal. **51**(3), 1777–1804 (2013)
14. Erath, C., Praetorius, D.: Adaptive vertex-centered finite volume methods with convergence rates. SIAM J. Numer. Anal. arXiv:1508.06155v2 (2016, preprint)
15. Ewing, R.E., Lin, T., Lin, Y.: On the accuracy of the finite volume element method based on piecewise linear polynomials. SIAM J. Numer. Anal. **39**(6), 1865–1888 (2002)
16. Feischl, M., Führer, T., Karkulik, M., Praetorius, D.: Stability of symmetric and nonsymmetric FEM–BEM couplings for nonlinear elasticity problems. Numer. Math. **130**(2), 199–223 (2015)
17. Gatica, G.N., Hsiao, G.C., Sayas, F.-J.: Relaxing the hypotheses of Bielak-MacCamy's BEM-FEM coupling. Numer. Math. **120**(3), 465–487 (2012)
18. Hackbusch, W.: On first and second order box schemes. Computing **41**(4), 277–296 (1989)
19. Heuer, N., Sayas, F.-J.: Analysis of a non-symmetric coupling of interior penalty DG and BEM. Math. Comput. **84**(292), 581–598 (2015)
20. Johnson, C., Nédélec, J.C.: On the coupling of boundary integral and finite element methods. Math. Comput. **35**(152), 1063–1079 (1980)
21. McLean, W.: Strongly Elliptic Systems and Boundary Integral Equations. Cambridge University Press, Cambridge (2000)
22. Of, G., Steinbach, O.: Is the one-equation coupling of finite and boundary element methods always stable? Z. Angew. Math. Mech. **93**(6–7), 476–484 (2013)
23. Of, G., Steinbach, O.: On the ellipticity of coupled finite element and one-equation boundary element methods for boundary value problems. Numer. Math. **127**(3), 567–593 (2014)
24. Roos, H.G., Stynes, M., Tobiska, L.: Numerical Methods for Singularly Perturbed Differential Equations, vol. 24. Springer, Berlin (1996)
25. Sayas, F.-J.: The validity of Johnson–Nédélec's BEM–FEM coupling on polygonal interfaces. SIAM J. Numer. Anal. **47**(5), 3451–3463 (2009)
26. Sayas, F.-J.: The validity of Johnson–Nédélec's BEM–FEM coupling on polygonal interfaces. SIAM Rev. **55**(1), 131–146 (2013)
27. Steinbach, O.: A note on the stable one-equation coupling of finite and boundary elements. SIAM J. Numer. Anal. **49**(4), 1521–1531 (2011)

28. Steinbach, O.: On the stability of the non-symmetric BEM/FEM coupling in linear elasticity. Comput. Mech. **51**(4), 421–430 (2013)
29. Steinbach, O., Wendland, W.L.: On C. Neumann's method for second-order elliptic systems in domains with non-smooth boundaries. J. Math. Anal. Appl. **262**(2), 733–748 (2001)